Fractional diffusion model for force distribution in static granular media

W. L. Vargas*
Centro Internacional de Física, Bogotá, Colombia
and School of Engineering, Universidad Militar Nueva Granada, Bogotá, Colombia

J. C. Murcia, L. E. Palacio, and D. M. Dominguez
School of Engineering, Universidad Militar Nueva Granada, Bogotá, Colombia
(Received 20 January 2003; revised manuscript received 22 May 2003; published 11 August 2003)

We present the results of a numerical and an experimental investigation of the probability distribution of normal contact forces in static packs of particles with two different hardnesses. Force distributions are computed and compared with existing models and experimental data. It is found that the probability distribution function of normal contact forces $P(f)$ is well described by a semiempirical model derived from a fractional diffusion equation. This model reproduces most of the features common to force distributions observed in experimental and numerical studies including the finite value for $P(f)$ as the forces tend to zero. The results indicate that the fractional model fits well both the numerical and experimental data over a wide range of particle deformations in contrast to the existing models. These results provide an insight into the physics of granular media and complement previous findings.

DOI: 10.1103/PhysRevE.68.021302 PACS number(s): 83.80.Fg, 45.10.Hj, 05.10.Gg, 05.30.Pr

I. INTRODUCTION

It is now well established that the forces within granular media are distributed following a highly nonlinear network of stressed chains of particles. The forces above the average are concentrated in a network of ''force chains'' that carry most of the imposed load, while some particles within the bed are practically isolated from their neighbors and carry no load at all. An example of this network is shown in Fig. 1. Because the interparticle forces and their distribution determine the bulk properties of a granular system, this behavior has very important consequences in transport phenomena such as heat conduction [1,2], sound propagation [3–5], and electric conduction [6].

A common way to analyze the distribution of forces in granular materials is to determine the probability distribution function $P(f)$ of normal forces $f=F/\langle F\rangle$, between neighboring particles, where $\langle F\rangle$ indicates an ensemble average. The force distributions in granular media exhibit several common features. Experimental [7–9] and numerical [10–13] studies have shown that the probability density function (PDF) decays in an exponential manner for forces above the average, i.e., $f>1$ and has a peak and/or a plateau around the mean force $f\approx 1$. Recent molecular dynamics (MD) simulations with different static coefficients of friction between particles indicated that both distribution functions of normal and tangential forces are weakly dependent on particle friction with some features of forces well below the average that depend on μ [12]. These main features in the behavior of $P(f)$ are the same for both two- and three-dimensional packings [10]. Functional forms, both empirical [8] and theoretical [14], have been proposed to model the force distribution. In the limit of $f\to\infty$, these models predict an exponential force distribution, i.e., $P(f)\propto e^{-f}$. The behavior in the limit $f\to 0$ remains in controversy, however most of the experimental data indicate that $P(f)$ approaches a finite value. Several experimental [7,9,15] and numerical [16,10] studies have also indicated that the form of the stress distribution is a function of material properties, grain geometries, roughness, packing order, boundary geometries and aspect ratio of the confining vessel. Some studies have indicated a slow trend to Gaussian behavior at high loads [16,17] and even a crossover from exponential to Gaussian [18]; such a crossover, however, has not been observed experimentally. A simplified lattice model by Sexton *et al.* [19] indicates probability distribution functions for individual grains which appear Gaussian at all stages of loading.

In this paper, we report results and analyses on a simulation study of force distribution in two-dimensional (2D) granular packs under compression using a discrete element simulation (here taken to be synonymous with particle dynamics) and the statistical analysis of the force distribution in such systems using a fractional diffusion equation. In particular, we compare numerical and experimental data with predictions by the q model of Coppersmith *et al.* [14], the empirical model by Mueth *et al.* [8], and the predicted values by the fractional diffusion model. This study is similar in spirit to earlier studies of force distribution in dense two-dimensional granular systems, but differs primarily in the fact that tools from *fractional calculus* are used to describe the probability density function $P(f)$ of force distribution.

We determine $P(f)$ for two different sets of packings composed of either elastomeric (soft) or steel (hard) particles that had settled onto a planar base under the action of gravity and/or an imposed external load and compared them with a fractional diffusion equation aimed to describe the anomalous behavior. We show that the force distribution in these granular systems can be well described by applying the tools of fractional calculus in the modeling of the force statistics. The results indicate that the evolution of the force distribution with loading is not toward a more Gaussian behavior but instead the behavior becomes more anomalous (non-

*Corresponding author.
Electronic address: wvargas@007mundo.com

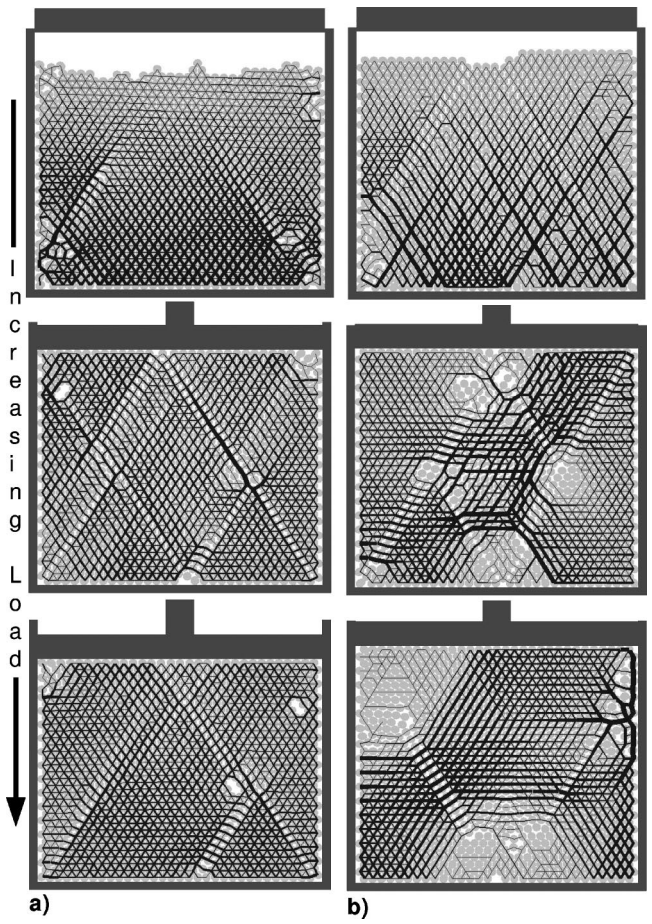

FIG. 1. Network of normal forces in a 2D packed bed as a function of imposed load. (a) Elastomeric particles $F=0$, 0.5, and 3 N, respectively. (b) Steel particles with $F=0$, 490, and 2000 N, respectively. Thicker intercenter lines correspond to larger forces. $F=0$ indicates that only hydrostatic pressure due to gravity has been imposed.

Gaussian) as the load is increased in agreement with recent experimental observations by Erikson *et al.* [7]. Fractional diffusion equations aimed at describing anomalous transport have been recently employed to investigate phenomena ranging from advection of particle tracers in porous media [20], fractional Brownian motion [21], anomalous diffusion with adsorption [22], fractional heat conduction [23], to tracer advection [24]. Closely related models have also been extensively used in the description of economic time series and market dynamics [25,26]. For a review on the subject the reader is referred to Ref. [27], and references therein.

The paper is organized as follows. Section II introduces the numerical method used in the study. The statistical tools are considered in Sec. III. In Sec. IV, we present numerical results for the stress propagation during a 2D quasistatic compression test and compare them with the predictions of a half fractional diffusion model. A comparison with the existing models and experimental data is also examined in this section. Finally, in Sec. V we provide conclusions and perspectives.

II. SIMULATION METHOD

Particle dynamics (PD) captures the macroscopic mechanical behavior of a particulate system via calculation of the trajectories of each of the individual particles within the mass. The time evolution of these trajectories, which are obtained via explicit solution of Newton's equations of motion for every particle, then determines the global flow of the granular material [28]. In a (soft-particle) PD simulation, the forces on the particles—aside from gravity—typically are determined from contact mechanics considerations [29]. In their simplest form, these relations include normal (Hertzian [30]) repulsion and some approximation of tangential friction (due to Mindlin [31]). A thorough description of possible interaction laws can be found in Refs. [32–34]; therefore they will not be reviewed here.

The method is based on the most basic mechanism of the constitutive phenomena in a granular assemble, that is, particle-to-particle interactions at contact points. To determine the translational and rotational motion of the particles in the assembly the classical Newtonian mechanics is used. The equations that describe the particle motion are

$$m_i \frac{d\mathbf{v}_i}{dt} = -m_i \mathbf{g} + \sum_{j=1} \mathbf{F}_c \tag{1}$$

for linear motion and

$$I_i \frac{d\boldsymbol{\omega}_i}{dt} = \sum_{j=1} |\mathbf{F}_t| \otimes \mathbf{r} \tag{2}$$

for angular motion, where $\mathbf{F}_c = \mathbf{F}_n + \mathbf{F}_t$, $\mathbf{F}_c$, being the total contact force, with $\mathbf{F}_n$, and $\mathbf{F}_t$ corresponding to the normal and the tangential force, respectively. The particle-to-particle interaction is established by allowing the assumed soft particles to overlap at the contact point. This overlap serves as a parameter in contact mechanics models used to determine the resultant contact force $\mathbf{F}_c$. The key feature of a PD simulation is that many simultaneous two-body interactions may be used to model a many-body system [28] and Eq. (1) may be used to evaluate their next position. This idea works because the time-step is chosen to be sufficiently small such that any disturbance (in this case a displacement-induced stress on a particle) does not propagate further than that particle's immediate neighbors within one time step. Generally, this criterion is met by choosing a time step which is smaller than r/λ, where r is the particle radius and λ represents the relevant disturbance wave speed (for example, dilational, distortional, or Rayleigh waves [35]). In general, the relevant wave speed is

$$\lambda \propto \sqrt{\frac{E}{\rho}}, \tag{3}$$

which for steel yields a time step of $\approx 10^{-6}$ s and for elastomeric particles $\approx 10^{-4}$ s. This latest time step is too large for PD to be stable, therefore this value was multiplied by a constant to yield a time step of the order of 10^{-7} s. Under these conditions, the method becomes explicit, and, there-

TABLE I. Parameters used in the simulations.

Parameter	Elastomer	Steel
Density kg/m^3	1250	7900
Poisson ratio	0.36	0.29
Young's modulus (GPa)	3.15×10^{-6}	193
Applied load (N)	0–3	0–2000
Number of particles	1032	
Particle diameter d_p (m)	0.01	
Length (m)	$30d_p$	
Height (m)	$30d_p$	
Friction coefficient μ	0.29	
Damping coefficient	1.0×10^{-4}	

fore, at any time increment the resultant forces on any particle are determined exclusively by its interaction with the closest neighbors in contact. With the accelerations known (both linear and rotational), the velocities and displacements may be obtained by numerical integration using a finite differences scheme.

The simulation consists of a monodisperse system of perfectly smooth noncohesive spheres forming a regular two-dimensional pseudoregular packed bed (one-particle deep), compressed by a wall of known weight. All material properties are taken directly from the literature and consist solely of the mechanical properties of the solids (see Table I). A typical initial condition for simulation is obtained by perturbing a hexagonal lattice (by removing random particles from the lattice) and allowing them to resettle under gravity. Particles settle onto a planar bottom wall under the action of a wall loaded by a constant force. The frictional and elastic properties of the wall are those characteristic of steel. The compression test was considered complete when the kinetic energy of the compressive wall reaches a threshold value close to zero and the system a quasistatic equilibrium.

III. A FRACTIONAL DIFFUSION EQUATION FOR FORCE DISTRIBUTION

Visualization of two-dimensional granular systems applying stress-induced birefringence as well as results coming from numerical studies (similar to those displayed in Fig. 1) demonstrate that forces within granular media follow preferred paths, the so-called stress chains or force chains network. Stress chains belong to an interesting class of complex branching networks, which are not only of intrinsic scientific interest but also a pervasive natural phenomenon. Such branching networks have been observed in the Internet [36], the vascular system [37–39], river networks [40–42], drainage networks [43], traffic flow [44], and the connectivity of the brain [45,46]. Common to all these different problems is the presence of a power law scaling, tailed distributions, and memory effects. At present, there is no generally accepted theory for explaining the origin of such a behavior. One recent form of describing these observations is the use of stochastic approaches based on fractional kinetic equations [27,47–52]. In particular, for granular media under loading, the probability distribution functions that can be derived from a fractional kinetic equation [53] not only possess all the main features that have been observed both in experimental and computational studies of sphere packings but also describe observations indicating that granular media appear to organize itself in a way that its force distribution lies in between the totally random (Gaussian) and the highly correlated limits (non-Gaussian) [54]. Both issues provide motivation for using fractional derivatives in an attempt to describe the force distribution within granular media. In addition, the present model draws inspiration not only from the observations common to complex branching networks, as discussed above, but also is based on ideas previously applied by Oda [55] and Antony [13] who used Gaussian-like distributions for the description of the probability distribution function of normal forces. Here, the probability distribution function $P(f)$ is described by a differential equation of the form

$$\frac{\partial^\beta P}{\partial z^\beta} = D\frac{\partial^\alpha P}{\partial f^\alpha} + \frac{z^{-\beta}}{\Gamma(1-\beta)}\delta(f). \tag{4}$$

Equation (4) is a diffusion type of equation, where time has been replaced by the z coordinate and the spatial coordinate by the normalized force f. The ''diffusion constant'' D is assumed to be independent of z. Persson [56] used a similar reasoning on his study of adhesion between an elastic body and a randomly rough hard surface. In Eq. (4) the operator $\partial^\beta/\partial z^\beta$ is the fractional Riemann-Liouville time derivative of the order of β and $\partial^\alpha/\partial f^\alpha$ is the Riesz space fractional derivative of order α. These fractional derivatives are integro-differential operators whose definition is given in Refs. [48,57]. The last term in Eq. (4) is the source term and depends on the initial conditions. Most of the studies use free boundary conditions and initial conditions centered on the origin, i.e., $P(f,0)=\delta(f)$, such that the Fourier-Laplace transforms of the Green functions [i.e., the solution for the $\delta(f)$ initial condition $P(f,0)=\delta(f)$] can be easily obtained. Two particular cases are important to this study, the case of $0<\beta\leqslant 1$ and $\alpha=2$ that corresponds to the so-called fractal Brownian motion or time-fractional diffusion equation and $\alpha=\beta$ which denotes the case of neutral fractional diffusion. Following the results by Mainardi *et al.* [53,58], Eq. (4) becomes, for the case of the *time-fractional diffusion equation*, equivalent to the following initial value problem

$$\frac{\partial^\beta P}{\partial z^\beta} = D\frac{\partial^2 P}{\partial f^2} + \frac{z^{-\beta}}{\Gamma(1-\beta)}\delta(f), \tag{5}$$

where D denotes a positive constant with dimensions L^β. Solution of Eq. 5 with the initial condition $P(f,0)=\delta(f)$ is obtained by Fourier transforming both sides of the equation with respect to f. After integration and inverse Fourier transforming of the Green function, the solution is given by

$$P(f,z) = \frac{1}{2\sqrt{D}z^\nu}K(\zeta,\nu), \tag{6}$$

where $\nu=\beta/2.0$ and $K(\zeta,\nu)$ is a function of Wright type, defined by

$$K(\zeta,\nu)=\frac{1}{\pi}\sum_{n=0}^{\infty}\frac{(-\zeta)^{n-1}}{(n-1)!}\Gamma(n\nu)\sin(n\pi\nu), \tag{7}$$

with

$$\zeta=\frac{f}{\sqrt{D}z^{\nu}}. \tag{8}$$

The classical Gaussian solution is recovered when $\nu=0.5$. The properties of the $K(\zeta,\alpha)$ function are given in Refs. [53,57]. It can be shown [53] that Eq. (6) can be interpreted as a symmetric distribution evolving in z, with a stretched exponential decay, i.e., $P(f,1)\approx af^{b}\exp(-cf^{d})$ as $f\rightarrow\infty$. Note the similarities of this form with the q model by Coppersmith *et al.* [14].

The case of *neutral fractional diffusion* which includes the Cauchy diffusion problem, i.e., $\beta=\alpha=1$ and the limiting case of wave propagation for $\beta=\alpha=2$, can be solved following similar procedures as outlined above [53]. The solution to this problem is given by

$$P(f,z)=\frac{1}{2(Dz)}K(\zeta,\alpha), \tag{9}$$

with

$$K(\zeta,\alpha)=\frac{1}{\pi}\frac{f^{\alpha-1}\sin\left[\frac{\pi}{2}\alpha\right]}{1+2f^{\alpha}\cos\left[\frac{\pi}{2}\alpha\right]+f^{2\alpha}}, \tag{10}$$

ζ is given in this case by

$$\zeta=\frac{f}{(Dz)}. \tag{11}$$

The probability distribution functions obtained in Eqs. (6) and (9) above have a generalized scaling form

$$P(f,z)=z^{-\gamma}K(f/z^{\gamma}), \tag{12}$$

where $\gamma=\beta/\alpha$ is the anomalous diffusion exponent which can be viewed as a measure of the long-range correlation in the force dispersion and with f/z^{γ} being a similarity variable. Equation (12) resembles similar expressions used to describe the Lagrangian dynamics of particle displacements under flow conditions [59,60]. A similar scaling function was used by Coppersmith *et al.* [14] in the derivation of the so-called q model.

IV. RESULTS AND DISCUSSION

Figures 1(a) and 1(b) show the evolution of the networks of normal contact forces for both elastomeric and steel particles, respectively, at three different levels of loading. It is observed for both systems that a subnetwork of stress chains carries most of the applied external load in agreement with previous experimental [15,61] and computational [1,10,11] studies. The percentage of deformation in this study covers a range from 6% up to 25% for the elastomeric particles and from 0.5% to 2.5% for the steel particles. The thickness of the intercenter lines, which indicates the force carried by particles in contact, shows that the contact-to-contact fluctuations is less pronounced for a system with elastomeric particles. Qualitatively, the number of particles which carry small forces (thinner lines) appear to be lower in the system with soft particles [Fig. 1(a)] than in the bed with hard particles, Fig. 1(b).

Force distributions

Log-log plots of probability distributions of contact normal forces are shown in Figs. 2 and 3 for steel and elastomeric particles, respectively. For the particles of higher hardness (steel), Fig. 2 shows how the probability distribution function of contact normal forces evolves during a quasistatic compression test. All forces are normalized with respect to their average ($\langle F\rangle$) in each sample. The normalized probability distributions show that as the external load is increased the system response evolves from an almost perfect Gaussian distribution, for the granular packing that has been formed under a hydrostatic head [see Fig. 2(a)], to a non-Gaussian response at the highest load, Fig. 2(c). The numerical data show all the features previously reported, namely, a peak around the average, a plateau below the average force, and an exponential decay for forces above the average. The results in Fig. 2(a) with no external force are consistent with the experimental results by Løvoll *et al.* [62] using glass beads.

In Fig. 2 the dashed line corresponds to a PDF with a Gaussian distribution obtained by solving Eqs. (6)–(8) with $\alpha=2$, $\beta=1$, and $D=z=1$. The continuous line in Fig. 2 (b) is a fitting with Eqs. (6)–(8) with $\alpha=2$, $\beta=1.4$, and $D=z=1$. The solid line in Figure 2 (c) represents the solution of Eqs. (9)–(11) with $\alpha=\beta=1.7$, and $D=z=1$. The distribution function captures the exponential decay for forces above the average ($f>1$), the plateau of the distribution for forces below the average ($f<1$), and the peak around the mean ($f\approx1$). The results indicate both qualitatively (by the shape of the distribution) and quantitatively (by the β and α orders of the fractional diffusion equation) that the response of the system evolves from Gaussian to anomalous. Results with a larger system (15 000 particles)—not shown—indicate that increasing the system size has no effect on the results other than improving the statistics of the data.

In order to compare the behavior of particles with a high hardness with that of softer particles, a similar set of numerical experiments was performed using elastomeric particles. These results are shown in Fig. 3.

For softer particles, the results indicate that as the imposed load (degree of deformation) increases, the shape of the PDF departs from the Gaussian behavior which has been reported at large deformations. The soft elastomeric particles, which sustain a larger amount of deformation, show a more pronounced peak around the average ($f\approx1$) and a steeper decay. The results in Fig. 3 are in good qualitative agreement with the experimental observations of Erikson *et al.* [7] who

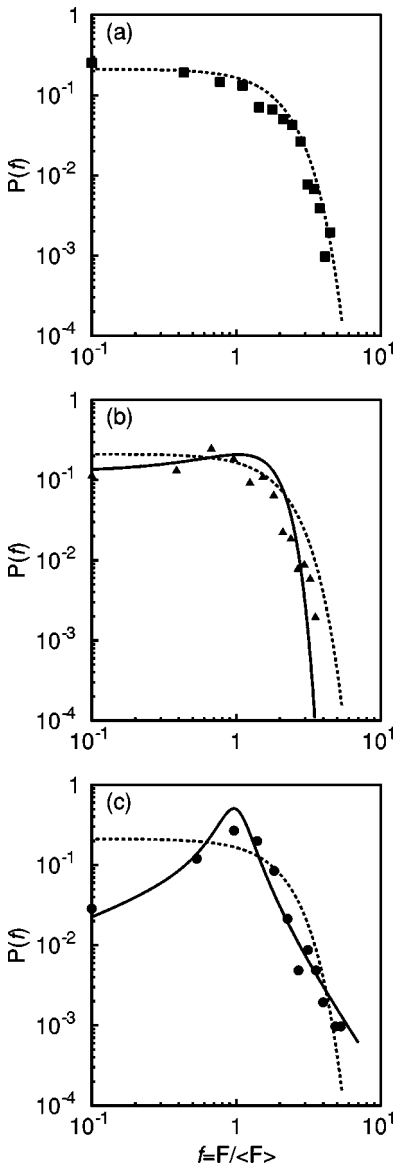

FIG. 2. Probability distribution function $P(f)$ of normalized normal forces as a function of applied load for steel beads. The panels shown correspond with an applied load of 0, 490, and 2000 N, respectively. The lines represent the solution of the fractional model. The dashed line corresponds to $\alpha=2,\beta=1$ which represents a normal Gaussian distribution. The continuous line represents a non-Gaussian distribution with (b) $\alpha=2$, $\beta=1.4$ and (c) $\alpha=\beta=1.7$, respectively. The fitting functions are explained in the text.

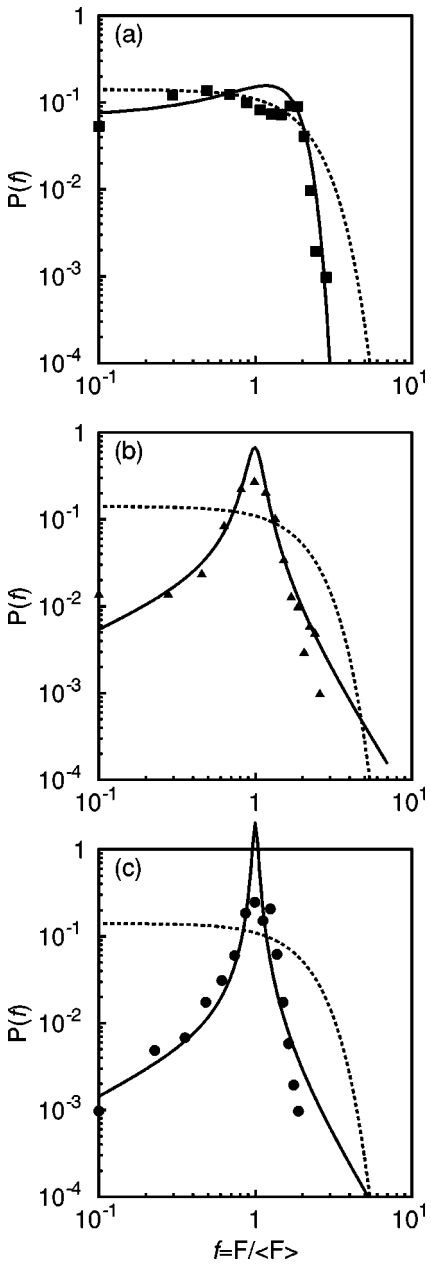

FIG. 3. Probability distribution function $P(f)$ of normalized normal forces as a function of applied load for soft elastomeric beads. The panels shown correspond with an applied load of 0, 0.5, and 3 N, respectively. The lines represent the solution of the fractional model. The dashed line corresponds to $\alpha=2,\beta=1$ which represents a normal Gaussian distribution. The continuous line corresponds to a non-Gaussian distribution with (a) $\alpha=2$, $\beta=1.5$, (b) $\alpha=\beta=1.85$, and (c) $\alpha=\beta=1.95$, respectively. The fitting functions are explained in the text.

used soft rubber particles. Once again, a transition from Gaussian to anomalous behavior is clearly observed. This result is confirmed by the orders of the fractional diffusion equation used to fit the data, which change from values close to a Gaussian distribution, i.e., $\beta\approx1$, and $\alpha\approx2$ to values that indicate a wavelike behavior, i.e., $\beta=\alpha=2$.

Similar to the dashed lines shown in Fig. 2, the dashed line in Fig. 3 corresponds to a PDF with a Gaussian distribution obtained by solving Eqs. (6)–(8) with $\alpha=2$, $\beta=1$, and $D=z=1$. The continuous line in Fig. 3(a) is a fitting with Eqs. (6)–(8) with $\alpha=2$, $\beta=1.5$, and $D=z=1$. The solid lines in Figs 3(b) and 3(c) represent the solution of Eqs. (9)–(11) with $D=z=1$, for $\alpha=\beta=1.85$ and $\alpha=\beta=1.95$, respectively.

The observations presented above indicate that, in many aspects, the quasistatic deformation of hard and soft particles is qualitatively similar. Starting with a distribution that closely resembles a Gaussian profile at low loads, the system evolves toward a non-Gaussian distribution that becomes more anomalous as the load is increased. There are, however,

some differences. While the particles with the higher hardness evolve from a Gaussian behavior to a time-fractional response and finally at high loads to a neutral-fractional response, the softer material response indicates a behavior which is anomalous from the very beginning and that can be best described with a time-fractional equation at low loads and at larger loads with a neutral-fractional diffusion equation. In agreement with recent experimental observations [7], our results indicate a non-Gaussian decay. The distributions decay exponentially and even slower at forces above the average and for large degrees of deformation.

It is known that the microstructure within granular media is modified by even the smallest amount of disorder, e.g., polydispersity in size or shape and the presence of roughness, so that, ultimately, the individual particle properties play a fundamental role in determining the bulk behavior of a granular system. In particular, the probability distribution function of contact forces is strongly influenced by the contact mechanics exhibited by the particles [2]. In this study the simulations have been carried out using smooth spherical particles, therefore, some of the the results discussed above might not represent a universal behavior. This implies that changes in parameters that can affect the microstructure of the pack will have an effect on the $P(f)$ profiles. This issue remains to be explored.

Comparison with existing models

Up to this point it has been shown that predictions of the fractional model when compared with numerical data for particles with two different hardnesses are in good qualitative agreement. In this section we compare the predictions of the fractional model with well established models. To compare experimental and/or numerical calculated data on $P(f)$ with the predictions of theoretical or empirical models, two functional forms have extensively been used, the so-called q model by Coppersmith *et al.* [14] and the empirical model proposed by Mueth *et al.* [8]. Adopting a stochastic perspective, a mean-field solution for the probability distribution of normal contact forces was derived by Coppersmith *et al.* [14]. The q model has the form

$$P(f)=\frac{k^k}{(k-1)!}f^{k-1}\exp(-kf), \tag{13}$$

where $f=F/\langle F\rangle$ is the normalized normal contact force. Mueth *et al.* [8] proposed a purely empirical model of the form

$$P(f)=a(1-be^{-f^2})e^{\beta f}, \tag{14}$$

where a, b, and β are fitting constants. A slightly generalized version of Eq. (14) has been used in Ref. [9]. This functional form is written as

$$P(f)=a(1-be^{-cf^2})e^{df}, \tag{15}$$

where a, b, c, and d are also fitting constants. The two functional forms in Eqs. (14) and (15) capture all the features common to force distributions in granular media, that is, the exponential tail at large f, the plateau near $f\approx 1$, the upturn in $P(f)$ as $f\to 0$, as well as the finite value of $P(f)$ as $f\to 0$. To compare the predictions of the proposed fractional model with the existing models, we fit Eqs. (13) and (15) to our numerical data for the system with the highest degree of deformation. These numerical data correspond with those in Figs. 2(c) and 3(c). The results of this exercise are shown in Fig. 4.

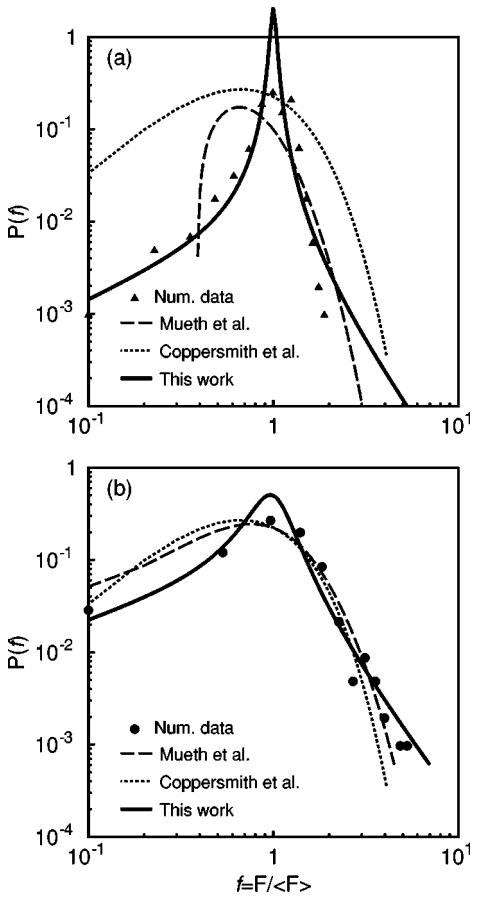

FIG. 4. A comparison of probability distribution function models with numerical data. (a) Elastomeric particles for $F=3$ N. The dotted line represents a fit with Eq. (13), $k=3$. The dashed line corresponds to Eq. (15) using $a=4.0$, $b=1.35$, $c=2.0$, and $d=3.5$. (b) Steel particles for $F=2000$ N. Dotted line same as in panel (a). The dashed line corresponds to Eq. (15) using $a=2.0$, $b=0.98$, $c=1.1$, and $d=1.8$. The solid lines are fittings with the fractional model Eqs. (9)–(11) with (a) $D=z=1$, $\alpha=\beta=1.95$ (b) $D=z=1$, $\alpha=\beta=1.7$

Figures 4(a) and 4(b) show the contact force distribution obtained for ''soft'' and ''hard'' particles, corresponding to a degree of deformation of 24.9% and 2.4%, respectively. The lines indicate the three different models used for comparison and full symbols the numerical data. The dotted line represents the predictions based on the theoretical model given by Eq. (13) with $k=3$. The results indicate that this model fits very poorly with the numerical data as the degree of deformation increases significantly, that is, as we go from Fig. 4(b) to 4(a). For the system with a low degree of deformation [Fig. 4(b)], the q model properly captures the exponential decay for forces well above the average, but fails to capture

the distribution for forces below the average. In agreement with previous studies we find for both soft and hard materials that $P(f)$ does not approach zero as $f \to 0$, in contrast with the predictions of the q model in Eq. (13). In the context of a toy model, Sexton *et al.* [19] concluded that for bead packs in which particles suffer a large deformation, the predictions based on the q model might be inaccurate and, therefore, this model could only be a good approximation for weak compression regimes. The results in Fig. 4 seem to confirm these conclusions. A recent numerical study by Snoeijer *et al.* [63] indicates that the discrepancies between the q model and experimental and/or numerical data might be due to differences in the contact geometry; this argument however still needs to be tested experimentally.

The dashed lines in Fig. 4(a), which correspond to the empirical fit of Eq. (15), indicate that the agreement between the model and numerical data is poor for most of $P(f)$, only a marginal agreement on the behavior of $P(f)$ for large values of f is achieved with the best fitting parameters. The empirical fit of Eq. (15), in Fig. 4(b), indicates a moderate agreement with the numerical data. The fit of Eq. (15) in this case is much better than in the case of the system of Fig. 4(a) whose degree of deformation is higher, suggesting that similar to the case of the q model, the empirical model of Mueth *et al.* [8] seems to perform better for systems with a low degree of deformation as that in panel Fig. 4(b). The fitting with the fractional model, Eqs. (9)–(11) here represented by the solid continuous lines, indicate a good agreement with the numerical data throughout the bulk of $P(f)$, but falling off less quickly than the numerical data for forces $f>1$ in the case of the system with the largest deformation in Fig. 4(a).

Comparison with experimental data

The predictions of our model as well as the numerical results can be easily tested using the now standard carbon paper technique developed by the authors of Refs. [7–9,64]. The granular packs studied are 3D packs of stainless steel beads with diameter $d=4.76\pm0.02$ mm and polymer pellets (polypropylene homopolymer, Rockwell hardness 96) with a $d_{eff}=3.17\pm0.1$ mm, respectively. The particles are confined in a steel cylinder of 150 mm in height and 75 mm inner diameter. Once the cylinder is filled with particles, a specified load is applied to the upper piston using a hydraulic press, while the lower piston is held fixed. The packs of polymer particles are constructed with one layer of steel particles at the bottom surface. Polymer particles are carefully added on top of the steel layer so as not to disturb the underlying steel beads. This arrangement facilitates the experimentation with the polymer particles whose shapes are fairly nonspherical. Contact forces are measured by lining the bottom piston with a layer of carbon paper with white glossy paper underneath. Steel beads at the bottom of the container press the carbon paper and leave marks whose darkness and area depend on the force applied on the bead. Once the load has been applied, the system is disassembled and the pattern of marks on the paper is digitized using a flatbed scanner for further image analysis. The force is determined by interpolation on calibration curves obtained by pressing a single particle with forces in the range of interest. All forces for a given experimental run are normalized using the average force for that run and the resulting probability distribution is the result of averaging three independent experimental runs. The results for steel and polymeric particles are shown in Fig. 5.

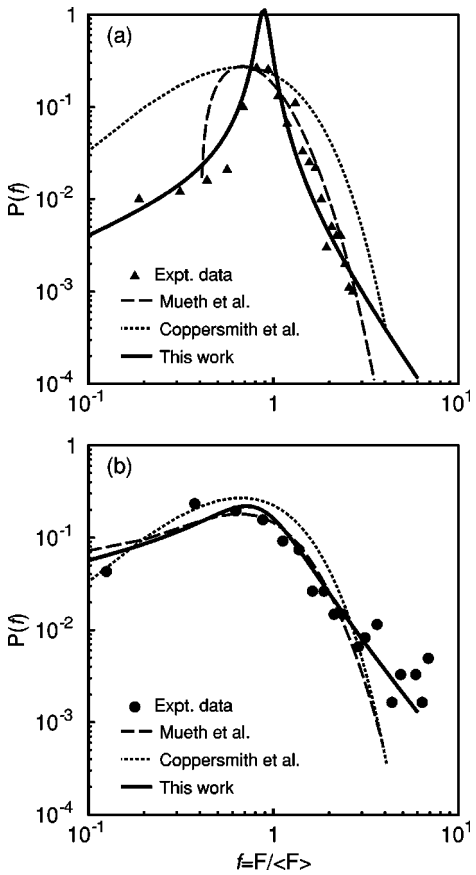

FIG. 5. Probability distribution function $P(f)$ obtained using the carbon paper technique (a) polymer particles for $F=800$ N and (b) steel particles for $F=800$ N. The dotted lines represents a fit with Eq. (13), $k=3$. The dashed line corresponds to Eq. (15) using (a) $a=4.0$, $b=1.5$, $c=2.5$, and $d=3.0$; (b) $a=1.4$, $b=0.95$, $c=1.4$ and $d=2.0$. The solid lines are fittings with the fractional model Eqs. (9)–(11) with (a) $D=0.4$, $z=1$, $\alpha=\beta=1.45$; (b) $D=0.4$, $z=1$, $\alpha=\beta=1.9$. The degree of deformation is (a) 11.5% and (b) 1.8%, respectively.

In Figure 5 we compare the PDF obtained from experiments with the predictions of the fractional model introduced in Sec. III and the two models for $P(f)$ in Eqs. (13) and (15), respectively. For both soft and hard particles we find that the shape of the experimentally determined $P(f)$ is qualitatively similar to those we observe in the simulations of the previous sections at similar levels of loading (see Fig. 4). These results are also in agreement with previous experimental findings [7]. When the experimental data is correlated with the functional forms for $P(f)$ in Eqs. (13) and (15), it is observed that the behavior is remarkably similar to that in Fig. 4. For the soft particles in Fig. 5(a), which sustained the largest degree of deformation both the q model and the generalized version of Mueth's empirical model fit poorly the experimental data. The q model properly predicts the trend

for forces above the average; the values, however, are overpredicted. The dashed line in Fig. 5, which corresponds to the empirical fit of Eq. (15), indicates that the agreement between the model and the experimental data is marginal for large values of f. Both models fail to capture the distribution for forces below the average. The fitting with the fractional model, Eqs. (9)–(11) here represented by the solid continuous line, indicates a good agreement with the experimental data but decaying slower than the experimental data, for forces $f>1$; also some overprediction of the peak value at $f\approx 1$ is observed. The results in Fig. 5(b), which correspond to the hard system, show that the fit with the q model and the empirical model in Eq. (15) are in moderate agreement with the experimental data, a significant deviation for forces well above the average is observed. Similar to the findings in the preceding section, we note that both models seem to perform better when applied to a system with a low degree of deformation. The fit with the fractional model in Eqs. (9)–(11) is good over the entire range of forces.

The results reported have demonstrated that a fractional diffusion equation fits reasonably well with the force distribution in granular media even for large levels of particle deformation therefore providing an alternative way to analyze force distribution functions. There are however, some difficulties with this model. In particular, the upturn observed in $P(f)$, both in simulations and experiments at small forces, is not well captured by the fractional model. However, the model predicts in all the cases a finite value of $P(f)$ as $f\rightarrow 0$ and observation that agrees quite well both with experimental and numerical findings [7,8,62]. Barkai [65], in his study on the foundations of the fractional diffusion equations, found that the fractional approximation can break down at the origin $f=0$, and, in general, the convergence of the solution at $f\rightarrow 0$ can be extremely slow. There are also difficulties to predict correctly the behavior of the high-order moments and, therefore, the solution might not describe properly the tails of the function, i.e., $f\rightarrow\infty$; similar observations have been put forward by Mainardi *et al.* [53]. These arguments might be the reason as to why the model does not capture properly the behavior at very small forces and for large values of f; further study into this problem is clearly required.

Recently, it has been pointed out by Claudin *et al.* [66] that an analogy between the results in the context of Lagrangian dynamics of particle tracers and stress propagation within granular media can be established. In particular, Lévy-like flights of particle tracers correspond in the present context to stress chains carrying heavy loads. Lévy flights in Lagrangian dynamics are believed to be responsible for the anomalous behavior of tracer diffusion [24,59]. It is likely that stress chains with forces well above the average have a similar effect on stress propagation. These observations and their analogy with Lagrangian dynamics certainly requires further exploration. The interested reader can refer to Refs. [59,60] for further details.

V. CONCLUSIONS AND OUTLOOK

In this paper, results have been presented for both numerical simulations and experiments of quasistatic compression of noncohesive systems of particles with two different hardnesses. It has been shown that for both soft (elastomeric) and hard (steel) particles the force distribution can be well described by a fractional diffusion equation. We find that the degree of deformation determines the orders of the fractional diffusion equation. At low deformations, either with hard or soft particles, the $P(f)$ follows a functionality that is close to a Gaussian distribution with $\beta\approx 1$ and $\alpha\approx 2$. As the deformation increases, the behavior becomes anomalous and $P(f)$ is asymmetric with tails that depart from a classical Gaussian distribution and reach a wavelike distribution with β and $\alpha\rightarrow 2$. The percentage of deformation in this study covers a range from 6% up to 25% for the elastomeric particles and from 0.5% to 2.5% for the steel particles. Our results support previous experimental observations [7] which indicate that for forces above the average the decay is non-Gaussian. These observations support the notion that a description based on a fractional diffusion equation might provide a useful tool to analyze force distributions in granular media; further work in this topic is clearly needed.

From a practical perspective, the observations in this study suggest that the addition of soft particles to packings of hard particles will modify the force distribution substantially. This simple modification in force transmission can have very important implications for practical uses such as improving the design of binders for plastic-bonded explosives and solid-rocket fuels, binders and fillers for asphalts, and hot spot reduction in chemical reactors among others. Our ongoing work will explore some of these topics.

ACKNOWLEDGMENTS

We thank the personnel of the Civil Engineering Department Laboratory (UMNG) for their assistance with the experimental measurements. We especially thank Dr. Eduardo Posada (CIF) for his continued interest and collaboration. The work of L.E.P., D.M.D. and J.C.M. has been supported by the *Research center* (School of Engineering-Universidad Militar Nueva Granada). J.C.M. has been financially supported in part by the Young Researchers Program of COLCIENCIAS-BID.

[1] W.L. Vargas and J.J. McCarthy, AIChE J. **47**, 1052 (2001).
[2] W.L. Vargas and J.J. McCarthy, Chem. Eng. Sci. **57**, 3119 (2002).
[3] C.H. Liu and S. Nagel, Phys. Rev. B **48**, 15 646 (1993).
[4] X. Jia, C. Caroli, and B. Velecky, Phys. Rev. Lett. **82**, 1863 (1999).
[5] D.L. Johnson, H.A. Makse, N. Gland, and L. Schwartz, Physica B **279**, 134 (2000).
[6] X. Zhuang, A.K. Didwania, and J.D. Goddard, J. Comput. Phys. **121**, 331 (1995).

[7] J.M. Erikson, N.W. Mueggenburg, H.M. Jaeger, and S.R. Nagel, Phys. Rev. E **66**, 040301(R) (2002).
[8] D.M. Mueth, H.J. Jaeger, and S.R. Nagel, Phys. Rev. E **57**, 3164 (1998).
[9] D.L. Blair, N.W. Mueggenburg, A.H. Marshall, H.M. Jaeger, and S.N. Nagel, cond-mat/0009313.
[10] F. Radjai, A. Roux, and J.J. Moreau, Chaos **9**, 544 (1999).
[11] F. Radjai, M. Jean, J.J. Moreau, and S. Roux, Phys. Rev. Lett. **77**, 274 (1996).
[12] L.E. Silbert, G.S. Grest, and J.W. Landry, Phys. Rev. E **66**, 061303 (2002).
[13] S.J. Antony, Phys. Rev. E **63**, 011302 (2001).
[14] S.N. Coppersmith, C.-H. Liu, S. Majumdar, O. Narayan, and T.A. Witten, Phys. Rev. E **53**, 4673 (1996).
[15] J. Geng, D. Howell, E. Longhi, R.P. Behringer, G. Raydellet, L. Vanel, E. Clément, and S. Ludig, Phys. Rev. Lett. **87**, 035506 (2001).
[16] C. Thornton and S.J. Anthony, Philos. Trans. R. Soc. London, Ser. A **356**, 2763 (1998).
[17] M.L. Nguyen and S.N. Coppersmith, e-print cond-mat/0005023.
[18] H.A. Makse, D.L. Johnson, and L.M. Schwartz, Phys. Rev. Lett. **84**, 4160 (2000).
[19] M.A. Sexton, J.E.S. Socolar, and D.G. Schaeffer, Phys. Rev. E **60**, 1999 (1999).
[20] D.A. Benson, Ph.D. thesis, University of Nevada, 1998 (unpublished).
[21] S.C. Lim and S.V. Muniandy, Phys. Rev. E **66**, 021114 (2002).
[22] G. Drazer, H.S. Wio, and C. Tsallis, Granular Matter **3**, 105 (2001).
[23] V.V. Kulish and J.L. Lage, J. Heat Transfer **122**, 372 (2000).
[24] W.L. Vargas, L.E. Palacio, and D.M. Dominguez, Phys. Rev. E **67**, 026314 (2003).
[25] N. Laskin, Physica A **287**, 482 (2000).
[26] E. Scalas, R. Gorenflo, and F. Mainardi, Physica A **284**, 376 (2000).
[27] R. Metzler and J. Klafter, Phys. Rep. **339**, 1 (2000).
[28] P.A. Cundall and O.D.L. Strack, Geotechnique **29**, 47 (1979).
[29] K.L. Johnson, *Contact Mechanics* (Cambridge University Press, Cambridge, 1987).
[30] H. Hertz, J. Reine Angew. Math. **92**, 1 (1881).
[31] R.D. Mindlin, J. Appl. Mech. **16**, 256 (1949).
[32] O. Walton and R.L. Braun, J. Rheol. **30**, 949 (1986).
[33] C. Thornton and K.K. Yin, Powder Technol. **65**, 153 (1991).
[34] J.J. McCarthy and J.M. Ottino, Powder Technol. **97**, 91 (1998).
[35] C. Thornton and C.W. Randall, *Micromechanics of Granular Material*, edited by M. Satake and J.T. Jenkins (Elsevier Science, Amsterdam, 1988), pp. 133–142.
[36] A.E. Motter and Y.-C. Lai, Phys. Rev. E **66**, 065102 (2002).
[37] G.B. West, J.M. Brown, and B.J. Enquist, Science **276**, 122 (1997).
[38] W. Huang, R.T. Yen, M. McLaurine, and G. Bledsoe, J. Appl. Physiol. **81**, 2123 (1996).
[39] D.L. Turcotte, J.D. Pelletier, and W.I. Newman, J. Theor. Biol. **193**, 577 (1998).
[40] P.S. Dodds and D.H. Rothman, Phys. Rev. E **63**, 016115 (2001).
[41] P.S. Dodds and D.H. Rothman, Phys. Rev. E **63**, 016116 (2001).
[42] P.S. Dodds and D.H. Rothman, Phys. Rev. E **63**, 016117 (2001).
[43] J.G. Masek and D.L. Turcotte, Earth Planet. Sci. Lett. **119**, 379 (1993).
[44] D. Helbing, Rev. Mod. Phys. **73**, 1067 (2001).
[45] C. Cherniak, M. Changizi, and D.W. Kang, Phys. Rev. E **59**, 6001 (1999).
[46] R. Segev, M. Benveniste, Y. Shapira, and E. Ben-Jacob, Phys. Rev. Lett. **90**, 168101 (2003).
[47] S. Jespersen, R. Metzler, and H.C. Fogedby, Phys. Rev. E **59**, 2736 (1999).
[48] R. Metzler and T.F. Nonnenmacher, Chem. Phys. **284**, 67 (2002).
[49] R. Hilfer, Fractals **11**, 251 (2003).
[50] A. Jurjiu, Ch. Friedrich, and A. Blumen, Chem. Phys. **284**, 221 (2002).
[51] N. Laskin, I. Lambadaris, F. Harmantzis, and M. Devetsikiotis (unpublished).
[52] A. Bazzani, G. Bassi, and G. Turchetti, Physica A **324**, 530 (2003).
[53] F. Mainardi, Y. Luchko, and G. Pagnini, Frac. Calc. Appl. Anal. **4**, 153 (2001).
[54] H.M. Jaeger, S.R. Nagel, and R.P. Behringer, Rev. Mod. Phys. **68**, 1259 (1996).
[55] M. Oda, Soils Found. **14**, 13 (1974).
[56] B.N.J. Persson, Eur. Phys. J. E **8**, 385 (2002).
[57] A.I. Saichev and G.M. Zaslavsky, Chaos **7**, 753 (1997).
[58] R. Gorenflo and F. Mainardi, Arch. Mech. **50**, 377 (1998).
[59] P. Castiglione, A. Mazzino, P. Muratore-Ginanneshi, and A. Vulpiani, Physica D **134**, 75 (1999).
[60] D. del Castillo-Negrete, Phys. Fluids **10**, 576 (1998).
[61] D.W. Howell, C.T. Veje, and R.P. Behringer, Chaos **9**, 559 (1999).
[62] G. Løvoll, K.J. Måløy, and E.G. Flekkøy, Phys. Rev. E **60**, 5872 (1999).
[63] J.H. Snoeijer, M. van Hecke, E. Somfai, and W. van Saarloos, Phys. Rev. E **67**, 030302(R) (2003).
[64] C.H. Liu, S. Nagel, D.A. Shecter, S.N. Coppersmith, S. Majumdar, O. Narayan, and T.A. Witten, Science **269**, 513 (1995).
[65] E. Barkai, Chem. Phys. **284**, 13 (2002).
[66] P. Claudin, J.-P. Bouchaud, M.E. Cates, and J.P. Wittmer, Phys. Rev. E **57**, 4441 (1998).